scientific reports

Check for updates

OPEN

Electrochemical measurement of morphine using a sensor fabricated from the CuS/g-C_3N_5/Ag nanocomposite

Hakimeh Teymourinia[1,2]✉, Zakyeh Akram[2], Ali Ramazani[1] & Vahid Amani[2]

Morphine, as one of the most important narcotic drugs, significantly affects the nervous system and increases euphoria, which raises the likelihood of its misuse. Therefore, its measurement is of great importance. In this work, a new electrochemical sensor based on a nanocomposite of CuS/g-C_3N_5/AgNPs was developed for modifying Screen printed carbon electrodes (SPCEs) and used for the measurement of morphine through cyclic voltammetry and differential pulse voltammetry. Various analytical methods initially characterized the nanocomposite. The prepared sensor, which also has an extensive surface area, achieved a detection limit of 0.01 µM for morphine in a concentration range of 0.05–100 µM at pH 7. Besides its excellent capability in measuring morphine in real samples, the sensor exhibits good stability, reproducibility, and repeatability. The presence of CuS, due to its excellent high surface area alongside silver nanoparticles, leads to an increase in the conductivity of the g-C_3N_5 modified electrode, resulting in an increased oxidative current of morphine at the surface of the prepared sensor. Therefore, measuring low concentrations of morphine with this sensor was made possible. Additionally, measuring morphine without interference from various species is a strong point of the electrochemical sensor for morphine detection, and combined with the simplicity and ease of the method, it allows for morphine measurements to be conducted in the shortest possible time.

Keywords Morphine, CuS, g-C_3N_5, AgNPs, Electrochemical measurement

Morphine (MO), originating from poppy plants, is a powerful narcotic medication mainly used to treat intense and long-lasting pain, particularly in patients with cancer. The drug is known for its therapeutic benefits such as providing pain relief, inducing relaxation, boosting energy, reducing coughing, and positively influencing several organ systems[1]. However, the consumption of MO is linked with a variety of possible negative effects, including a reduction in heart rate, respiratory insufficiency, disruptions in the central nervous system, risks of asphyxiation, and low blood pressure. Consuming too much MO can cause deadly respiratory failure[2]. Beyond these harmful physical impacts, such as potential teratogenic effects, MO is considered a dangerous narcotic and analgesic because it significantly alters the central nervous system's ability to transmit pain messages to the brain[3,4]. Dependency on MO can occur swiftly, often within a mere three days of beginning use[5]. As it is deemed an illicit drug, it is crucial to detect MO in different biological samples, underlining its significance in medical examinations and legal inquiries[2,6]. Thus, there is a pressing need to create a sensor that is sensitive, selective, and suitable for accurately measuring MO levels across various biological and environmental samples. A wide array of methods for the detection and measurement of MO is presented in the scientific literature, including techniques such as chromatographic assays[7], chemiluminescence[8], spectrophotometry[9], high-performance liquid chromatography (HPLC)[10,11], spectroscopy[12], fluorescence assays[13,14], and surface plasmon resonance[15]. Although some of these approaches offer considerable accuracy, they frequently come with limitations that restrict their practicality for immediate drug testing applications. Challenges include prohibitive costs, the absence of portability, the requirement for substantial time investments, and the need for specific laboratory apparatus in addition to steps for sample preparation before analysis. Recently, electrochemical techniques have risen to prominence as affordable, mobile, and uncomplicated approaches for the analysis of drugs, attracting considerable interest from the scientific community[16,17]. These techniques are noted for their high sensitivity, straightforwardness, and specificity, making electrochemical sensors indispensable tools for the identification of illegal drugs in biological materials. The advantages of these methods are manifold, including their precise

[1]Department of Chemistry, Faculty of Science, University of Zanjan, 45371-38791 Zanjan, Iran. [2]Department of Chemistry Education, Farhangian University, P.O. Box 14665-889, Tehran, Iran. ✉email: h.teymourinia@znu.ac.ir

selectivity, high accuracy, quick reaction times (just minutes), broad dynamic range, minimal detection levels, and user-friendliness[18,19]. However, the development of an effective and straightforward electrochemical sensor presents a notable challenge. Enhancing these sensors crucially involves creating a cost-effective, portable framework capable of the highly sensitive detection of particular substances. Key to this advancement is the modification of the electrode surface, which enables improvements in the sensor's sensitivity, precision, stability, and selectivity amidst significant external interference, while simultaneously lowering the detection limit (LOD)[20]. Moreover, it's essential to understand that MO is classified as a phenolic compound, capable of electron transfer to electrodes under certain potentials[21]. This property validates the use of electrochemical sensors as a viable platform for MO detection.

Screen printed carbon electrodes (SPCEs) are highly valued in the development of electrochemical sensors, as they offer a range of benefits that meet the requirements of modern analytical methods. Economical and scalable for production, they are perfectly suited for one-time use scenarios. The flexibility in their design permits a wide range of shapes, sizes, and electrode setups, making them adaptable to varied sensor needs. The single-use nature of SPCEs mitigates hygiene risks and prevents cross-contamination without necessitating thorough cleaning. Altering their surface enhances the sensitivity and selectivity for a broad range of analytes, essential in areas from environmental monitoring to medical diagnostics. SPCEs demand only small amounts of samples, boast portability for field analyses, are eco-friendly, and facilitate swift data acquisition. Such characteristics render SPCEs critical in the progression of fast and precise analytical and diagnostic methods[22–24]. To overcome these drawbacks, it's essential to enhance the SPCEs with modifiers that boast electrocatalytic properties. Graphitic carbon nitride emerges as a superior choice in this context, significantly boosting the electrode's operational efficiency and sensitivity.

Nitrogen-doped graphitic carbon nitride (g-C_3N_5) is recognized as a semiconductor material, distinguished by its distinct electronic and photophysical characteristics. The introduction of nitrogen improves its electrical conductivity, increases its surface area, and enhances its overall electronic features, making it a valuable modifier for electrodes used in the electrochemical analysis of substances[25]. In its role as an electrode substance, the nitrogen-enriched g-C_3N_4 demonstrates enhanced electrocatalytic capabilities, greater efficiency in charge transfer, and elevated levels of sensitivity and specificity for different analytes. Such improvements boost the efficacy of electrochemical sensors and biosensors, rendering them exceptionally adept at identifying and measuring various compounds in a range of environmental and biological contexts. Furthermore, the augmentation attributed to nitrogen incorporation not only reduces detection thresholds but also broadens the range of linear responses, markedly improving the effectiveness of electrochemical measurement approaches[26,27]. Employing copper sulfide (CuS) nanoparticles has been identified as a viable choice to improve the electrode's catalytic properties, sensitivity, electrical conductivity, and stability[28,29]. CuS nanoparticles has been recognized for its capabilities as a p-type semiconductor, making strides in fields such as the harvesting of solar energy, the development of LEDs, applications in photocatalysis, and the innovation of battery technologies[30–32]. The nanoparticle form of this substance has attracted attention due to its diverse morphologies, cost-effectiveness, enhanced catalytic properties, and improved electron mobility at the electrode surface. Such attributes render CuS nanoparticles an excellent choice for crafting electrochemical sensors, effectively marrying cost-efficiency with advanced technical performance[33,34]. In contrast to alternative CuS structures, the flower-like formation offers an increased specific surface area and a greater number of accessible active sites, enabling enhanced loading of electroactive species onto the electrode surface[35,36]. Additionally, the distinctive three-dimensional porous framework within the flower-like CuS facilitates swift analyte transport to the electrode interface, thereby augmenting the sensitivity and responsiveness of the electrochemical sensor[37,38]. In addition to the two previously mentioned modifiers, silver nanoparticles (AgNPs) have been shown to significantly improve the performance of electrodes in MO electrochemical sensors. Due to their high electrical conductivity and substantial surface area-to-volume ratio, AgNPs improve the electron transfer rate and offer numerous active sites for interaction with the analyte[39,40]. The integration of AgNPs into the electrodes can reduce the morphine oxidation overpotential compared to unmodified electrodes. Research indicates that the use of AgNPs on electrode surfaces can triple the current response and heighten the sensitivity for detecting MO. Moreover, AgNPs have the capacity to decrease interference from other substances, thereby enhancing the selectivity of the MO sensor in complex biological matrices[41,42].

Upon reviewing the published scientific literature, we found that a number of electrochemical sensors have been developed for the detection of MO. The study by Baghayeri et al. introduced a graphene/Ag nanoparticle-modified electrode capable of detecting methadone with a range of 1.0–200.0 μM and a low detection limit of 0.12 μM, showing promise for use in complex biological matrices like blood serum[41]. Beitollahi et al. created a graphene-cobalt oxide nanocomposite sensor with a detection range of 0.02–575.0 μM for MO, offering high selectivity over diclofenac and achieving near-perfect recovery in pharmaceutical and biological samples[43]. A colorimetric assay utilizing silver citrate-coated Au@Ag nanoparticles, which undergoes a color change for MO detection, has been created for its simplicity, stability, and selectivity, with optimization via variable-power sonication as noted by Bastami et al.[44]. Bastami et al. reported a colorimetric assay using Ag/Cu nanoparticles that discerns MO and methamphetamine by color change, with detection limits of 0.21 μg/mL and 0.49 μg/mL and incubation times of 7 and 35 min, respectively[42].

In this study, we developed a novel electrochemical sensor by modifying a SPCEs with g-C_3N_5, flower-like CuS nanoparticles, and Ag nanoparticles. The sensor was utilized to detect MO within biological specimens. Comprehensive characterization of the engineered composite material was conducted using multiple analytical methods, including, X-ray diffraction (XRD), energy dispersive X-ray spectroscopy (EDX), elemental analysis, and Field emission scanning electron microscopy (FE-SEM). Performance evaluation of the electrode was executed via cyclic voltammetry, examining influences of temperature, scan speed, morphine concentration,

and pH. For the quantitative determination of morphine in genuine biological matrices like plasma and urine, differential pulse voltammetry was employed.

Results

Characterization

The XRD pattern of g-C_3N_5 is shown in Fig. 1. It exhibits a broad peak at 2θ = 27°, corresponding to its aromatic structure's (002) planes. Figure 1 also shows the XRD pattern for CuS. The peaks are at 2θ = 27.5, 28.5, 29.4, 47, 54 and 61°. This indicates the successful synthesis of CuS. Figure 1 presents the XRD pattern of CuS/g-C_3N_5, where the CuS peaks remain visible. In the XRD pattern of nanocomposite CuS/g-C_3N_5/AgNPs, in addition to the CuS peaks, four other peaks are visible at 2θ = 35, 39, 61 and 78°. These correspond to silver nanoparticles (standard number JSCP-004) and are related to (111), (200), (220), and (311) planes. This confirms the successful synthesis of the CuS/g-C_3N_5/AgNPs nanocomposite[45–48].

Figure S1 shows FE-SEM images of CuS. The uniform size structures with self-assembled hexagonal nanoplates indicate the influence of Van der Waals forces, leading to the formation of nanoplate architectures. This growth process may be attributed to the end-to-end growth of plates, which is further enhanced by prolonged reaction time. These findings suggest that the formation of hexagonal nanoplates is likely influenced by the intrinsic anisotropic structural characteristics of CuS and the presence of the surfactant (CTAB). Additionally, the complete disappearance of tubular structures and the exclusive presence of self-assembled nanoplates further support this observation. It is well understood that nanostructures undergo nucleation and growth phases, and in the presence of a stabilizer such as CTAB, the growth phase is prolonged, preventing CuS nuclei from aggregating and resulting in the formation of nanoplates over an extended period of time. FE-SEM images of g-C_3N_5 are also visible in Figure S1, depicting nitrogen-rich carbon nitride as coarse plates with occasional rod-like structures. In the images of nanocomposites g-C_3N_5/CuS and CuS/g-C_3N_5/CdS, the CuS morphology

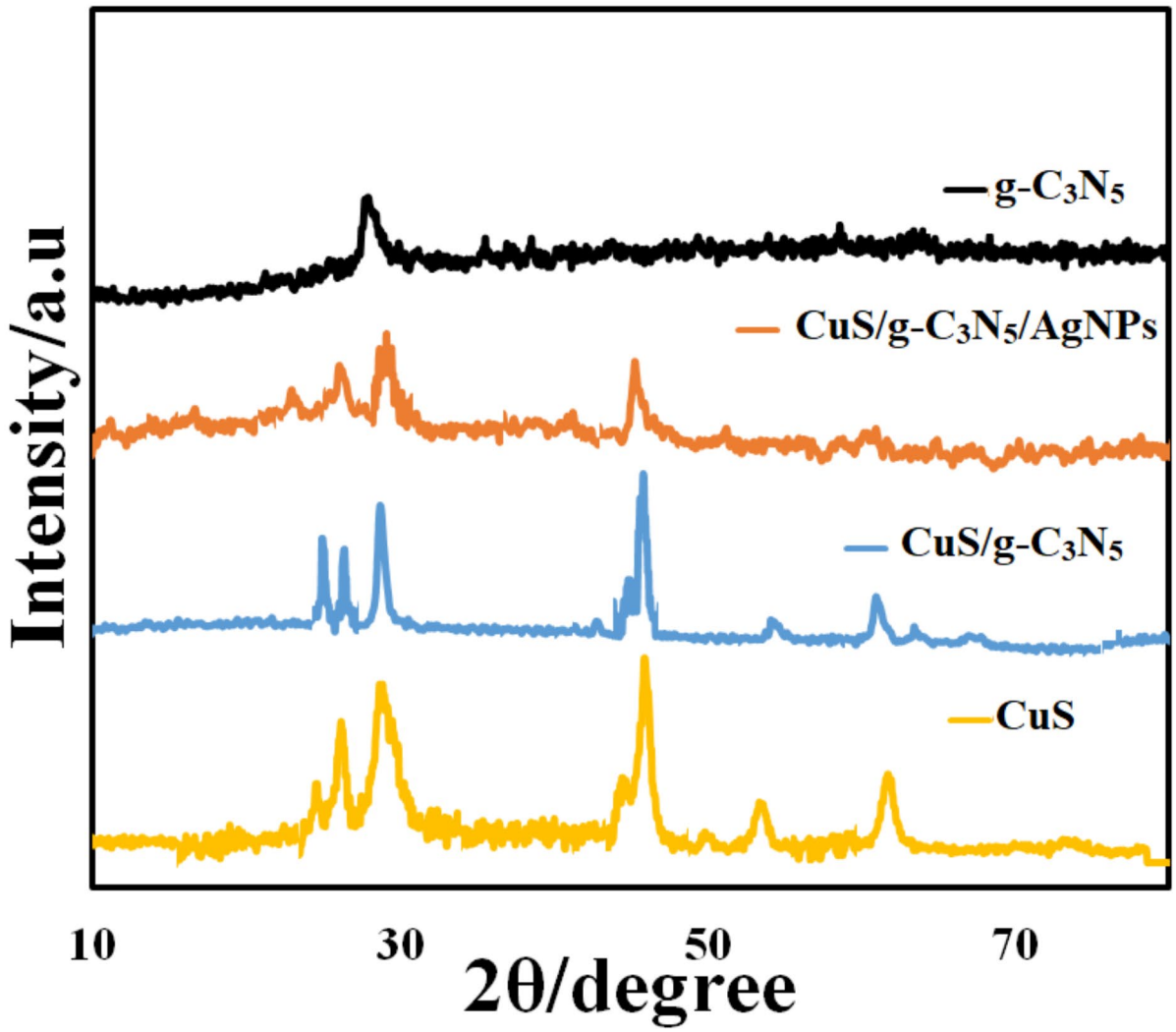

Fig. 1. XRD pattern of nanomaterial.

remains distinct as specific flower like, visible alongside g-C_3N_5. The presence of small silver nanoparticles is also discernible in the FE-SEM images[49–52].

Transmission electron microscopy images for the CuS/g-C_3N_5/AgNPs nanocomposite are presented in Fig. S2. These images clearly show CuS flower like, silver nanoparticles, and g-C_3N_5 structures. Figure S3 shows the elemental analysis of the CuS/g-C3N5/AgNPs nanocomposite, confirming its successful synthesis. This nanocomposite comprises the following elemental percentages: carbon (22.2%), nitrogen (15.11%), cupper (16.61%), and silver (28.94%).

Evaluation of electrode performance

The electrochemical performance of electrodes prepared in a potassium ferrocyanide/ferricyanide solution containing potassium chloride was investigated using electrochemical impedance spectroscopy. The results are presented in Fig. S4. The charge transfer resistance was found to be 1.83 KΩ for SPCE, 1.04 KΩ for SPCE/CuS, 0.85 KΩ for SPCE/g-C_3N_5, 0.3 KΩ for SPCE/CuS/g-C_3N_5 and 0.064 KΩ for SPCE/CuS/g-C_3N_5/AgNPs. Additionally, the electrochemical behavior of iron species on the surface of electrodes prepared in the potassium ferrocyanide/ferricyanide solution containing potassium chloride was examined using cyclic voltammetry. The oxidation/reduction potential differences for the iron species on the surfaces of electrodes SPCE, SPCE/CuS, SPCE/g-C_3N_5, SPCE/CuS/g-C_3N_5, and SPCE/CuS/g-C_3N_5/AgNPs were respectively found to be 0.28, 0.22, 0.23, 0.18 and 0.08 V. As observed, the charge transfer resistance and potential difference for the iron species on electrode e are lower compared to other electrodes, indicating better performance of this electrode. Furthermore, the surface area of the electrodes was investigated using the Randles-Sevcik equation. The obtained surface areas for SPCE, SPCE/CuS, SPCE/g-C_3N_5, SPCE/CuS/g-C_3N_5, and SPCE/CuS/g-C_3N_5/AgNPs were 0.036, 0.045, 0.048, 0.056 and 0.68 cm^{-1}, respectively. The study of the electrochemical behavior of morphine on the surfaces of SPCE, SPCE/CuS, SPCE/g-C_3N_5, SPCE/CuS/g-C_3N_5, and SPCE/CuS/g-C_3N_5/AgNPs was conducted using cyclic voltammetry in the potential window of 0 to 0.6 V. The voltammograms are presented in Fig. 2. An oxidative peak for morphine in a phosphate buffer solution with a pH of 7 is observed on the surfaces of the prepared electrodes. This oxidative peak for SPCE, SPCE/CuS, SPCE/g-C_3N_5, SPCE/CuS/g-C_3N_5, and SPCE/CuS/g-C_3N_5/AgNPs occurred respectively at potentials of 0.35, 0.35, 0.34, 0.33 and 0.32 V. Additionally, the oxidative current for 10 µM morphine at the surfaces of SPCE, SPCE/CuS, SPCE/g-C_3N_5, SPCE/CuS/g-C_3N_5, and SPCE/CuS/g-C_3N_5/AgNPs is respectively 0.5, 2, 3, 7.3, and 22 µA.

Therefore, the majority of the oxidative current is related to SPCE/CuS/g-C_3N_5/AgNPs. Additionally, the oxidative potential at the surface of SPCE/CuS/g-C_3N_5/AgNPs was observed to have more negative potentials than other electrodes. Hence, it can be said that SPCE/CuS/g-C_3N_5/AgNPs possesses electrocatalytic properties. This is due to the high surface area of SPCE/CuS/g-C_3N_5/AgNPs compared to different electrodes. Moreover, graphitic carbon nitride containing high levels of nitrogen (g-C_3N_5) increases the electrode surface area and enhances the conductivity of the unmodified electrode. On the other hand, CuS with a flower-like morphology significantly increases the electrode surface area due to its pristine morphology, which allows a more significant amount of analyte to be present on the electrode surface. Furthermore, silver increases the electrical conductivity of the electrode, consequently increasing the electron transfer rate and the oxidative current of morphine, and ultimately, electrocatalytic activity for SPCE/CuS/g-C_3N_5/AgNPs is observed, making it possible to measure morphine at lower concentrations[53,54].

Oxidation of morphine at different pH levels

In this study, the effect of pH as one of the most critical parameters affecting the potential and current of oxidation/reduction of various compounds was investigated using cyclic voltammetry. For this purpose, the measurement of morphine at surface SPCE/CuS/g-C_3N_5/AgNPs in a BR buffer solution at pH levels of 2, 3, 4, 5, 6, 7, 8, and 9 in the potential window of 0 to 0.6 V was conducted. The oxidative potential of morphine at pH levels of 2, 3, 4, 5, 6, 7, 8 and 9 occurred respectively at 0.58, 0.51, 0.45, 0.41, 0.38, 0.33, 0.28 and 0.33 V. The results indicate that with an increase in pH to alkaline values, a shift in potential towards more positive values occurred, and the slope of the line obtained from the pH versus potential graph is equivalent to the slope of the Nernst equation. Therefore, it can be said that the number of electrons/protons transferred in the electrochemical process of morphine is consistent. Additionally, the results show that the highest oxidative current is related to pH 7 (Fig. S5), thus this pH was selected as optimal. Furthermore, the morphine oxidation process is presented in Fig. 3.

Scan rate analysis

Investigating different scan rates is crucial for determining the electron transfer coefficient and the type of electrochemical process. Therefore, the oxidation of morphine at surface SPCE/CuS/g-C_3N_5/AgNPs was studied using cyclic voltammetry at various scan rates. The voltammograms of morphine at different scan rates are presented in Fig. S6. An increase in the oxidative current of morphine with increasing scan rate is observed; however, the oxidative peak of morphine is not well-defined at higher scan rates due to the insufficient opportunity for the species to reach the electrode surface, which prevents the precise observation of morphine oxidation. Since the electrochemical process is an electrocatalytic event, examining the type of reaction in the oxidation process of morphine is of great importance[46,55]. Figure S6b displays a plot of current versus the square of the scan rate, suggesting that the oxidation of morphine at surface SPCE/CuS/g-C_3N_5/AgNPs is a diffusion-controlled process. Additionally, to examine the electron transfer coefficient, a potential versus current plot at a scan rate of 10 mV at the starting potentials of the electrochemical process of morphine was drawn. The cathodic and anodic transfer coefficient αc is defined as -(RT/F)(dln|jc|/dE), where jc is the cathodic current density corrected for any changes in the reactant concentration on the electrode surface with respect to its bulk value, E is the applied electric potential, and R, T, and F have their usual significance. Based on the slope of Fig. S6c and cathodic and anodic transfer coefficient equation, an electron transfer coefficient of 0.55 was obtained.

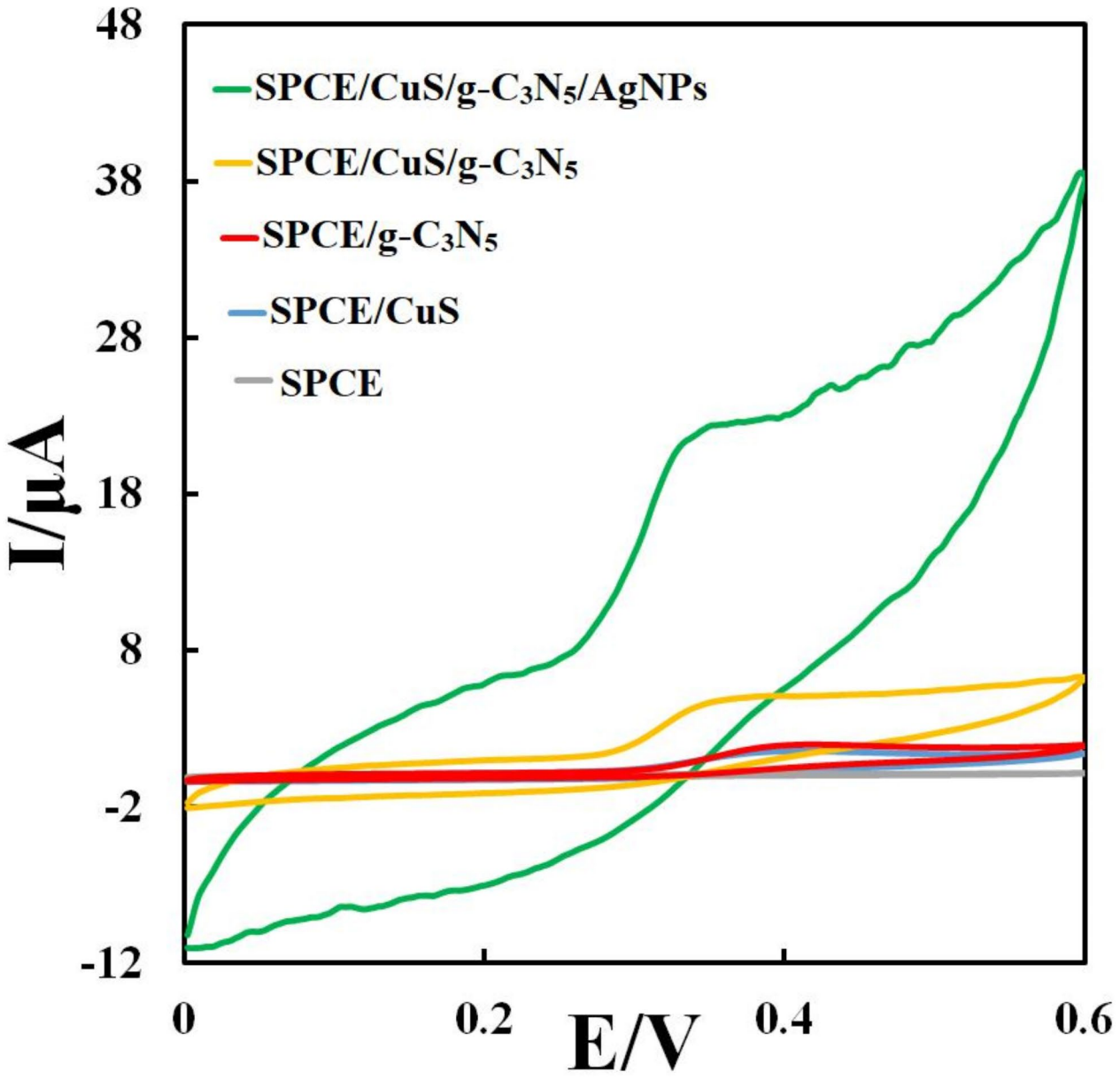

Fig. 2. CVs of 10 μM morphine at the surface electrodes.

Investigation of different concentrations

The investigation of different morphine concentrations at surface E was conducted using differential pulse voltammetry in the range of 0.05–150 μM in BR buffer solution with pH 7. The differential pulse voltammograms related to morphine are presented in Fig. S7. The increase in current is proportional to the concentration of morphine, which is confirmed by the graph observed in Fig. S7b. The limit of detection (LOD) obtained for morphine at surface SPCE/CuS/g-C_3N_5/AgNPs in the concentration range of 0.05–150 μM was determined using cathodic and anodic transfer coefficient equation s/m and found to be 0.01. A comparison of the performance of previous electrodes with the mentioned method for measuring morphine is provided in Table S1. The results indicate that the concentration range obtained here is broader, and the LOD for morphine using the sensor based on the modified electrode with e nanocomposite is equivalent and compared with other sensors. Therefore, the modified electrode demonstrated excellent capabilities in terms of LOD and concentration range, and it also exhibits good electrocatalytic activity alongside an easy synthesis method and unique and pristine morphology, which are distinctive features of this sensor.

Various compounds were used in the measurement of morphine to examine the selectivity of the method. The results are presented in Table S2. As the results show, various compounds have caused minor changes, less than 5%, in the oxidative current of morphine.

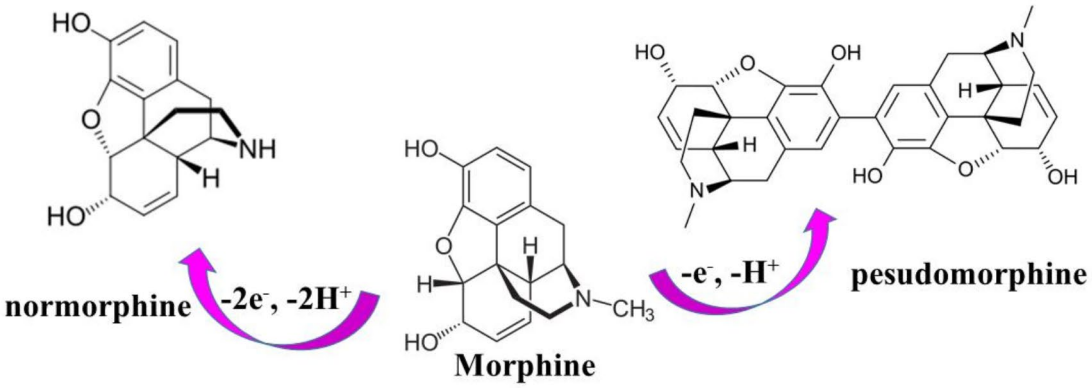

Fig. 3. The oxidation process of morphine.

The stability of the electrode fabricated based on nanocomposite e was investigated in a BR buffer solution with a pH of 7 over one month. The fabricated electrode was used weekly for morphine measurement, and each time after use, it was washed with water and buffer and stored at a temperature of 4 °C. The obtained relative standard deviation (RSD) value for the current obtained for the stability of the fabricated electrode was 3.94%, indicating good stability of the prepared sensor. The repeatability of the fabricated electrode was examined by measuring morphine four times consecutively. The obtained RSD value for the morphine currents over four consecutive repetitions was 3.21%, indicating good repeatability of the electrode. The reproducibility of the electrode was also carried out by modifying four electrodes similarly. The RSD value of the current obtained from the reproducibility of the electrode was 2.34%, which indicates good reproducibility of the prepared sensor.

Measurement of morphine in real sample

Morphine measurement in a real sample was conducted using a sensor prepared by the standard addition method at concentrations of 1, 5 and 10 in a blood sample. Table S3 shows that the recovery percentage obtained for morphine in the real sample at the mentioned concentrations ranges between 97 and 101%, and the RSD values for the real samples at these concentrations are 3.82%, 3.95%, and 3.62%.

Discussion

The measurement of morphine was carried out using an electrochemical sensor prepared based on CuS/g-C_3N_5/AgNPs nanocomposite, which has a high surface area and a unique and pristine morphology. Good results such as selectivity, stability, reproducibility, a wide concentration range, and a low detection limit comparable to other sensors were obtained in this work. The detection limit achieved in the 0.05–150 μM concentration range is 0.01 μM. Due to the presence of silver, flower-like Cus, and nitrogen-rich graphitic carbon nitride, the sensor prepared has shown excellent and remarkable results for the measurement of morphine. The modified electrode's meager charge transfer resistance, which indicates excellent conductivity and consequently increases the electron transfer rate at the electrode surface, is one of the exceptional characteristics of the prepared sensor. Therefore, the prepared sensor is recognized as a perfect sensor with outstanding features, and given that the prepared sensor has an exceptional capability for measuring morphine in blood plasma samples, it can also be used in medical applications. This electrochemical sensor was developed using cost-effective materials and synthesized through a novel and straightforward method that avoids the use of harmful solvents. Notably, the SPCE/CuS/g-C_3N_5/AgNPs demonstrates excellent performance in detecting morphine amidst various sample types, showcasing impressive selectivity for morphine analysis in real-world samples. Considering these advantages, the authors believe that the electrochemical sensor created with CuS/g-C_3N_5/AgNPs for improved signal amplification presents a viable approach for detecting morphine in real samples.

Methods

The materials and equipment, synthesis of CuS/g-C_3N_5/AgNPs nanocomposite, and preparation of electrochemical sensor with details are in Supplementary file.

Data availability

Data is provided within the manuscript or supplementary information files.

Received: 28 July 2024; Accepted: 1 November 2024
Published online: 09 November 2024

References

1. Ollikainen, E. et al. Rapid analysis of intraperitoneally administered morphine in mouse plasma and brain by microchip electrophoresis-electrochemical detection. *Sci. Rep.* **9** (1), 3311 (2019).
2. Imanzadeh, H. et al. Broken hollow carbon spheres decorated by gold nanodendrites as the advanced electrochemical sensing platform for sensitive tracing of morphine in human serum and saliva. *Sens. Actuators B.* **398**, 134738 (2024).
3. De, S., Choudhary, R. & Madhuri, R. *Determination of morphine in urine*. *Appl. Ion Exch. Mater. Biomedical Industries*, pp. 29–70 (2019).
4. Kadhem, A. A. & Alshamsi, H. A. *Biosynthesis of Ag-ZnO/rGO Nanocomposites Mediated Ceratophyllum demersum L. leaf Extract for Photocatalytic Degradation of Rhodamine B under Visible Light*1–15 (Biomass Conversion and Biorefinery, 2023).
5. Murphy, P. B., Bechmann, S. & Barrett, M. J. *Morphine* (2018).
6. Kish, S. S. et al. *Fabrication of a Novel Electrochemical Biosensor Based on easy and Efficient Modifications of a Glassy Carbon Electrode for Sensitive and Selective Determination of Morphine*, p. 40. 100555 (Sensing and Bio-Sensing Research, 2023).
7. Li, W. et al. Detection of saliva morphine using surface-enhanced Raman spectroscopy combined with immunochromatographic assay. *J. Raman Spectrosc.* **51**(4), 642–648 (2020).
8. Montgomery, M. T. et al. Extraction and determination of morphine present on the surface of Australian food grade poppy seeds using acidic potassium permanganate chemiluminescence detection. *Food. Anal. Methods*. **13**(5), 1159–1165 (2020).
9. Alshamsi, H. A. & Jabir, F. A. Green synthesis of Ni0. 5Zn0. 5O/TiO2 for photocatalytic, antibacterial and anticancer activities. *J. Mol. Liq.* **16**, 126037 (2024).
10. Tagliaro, F. et al. High-performance liquid chromatographic determination of morphine in biological samples: an overview of separation methods and detection techniques. *J. Chromatogr. B Biomed. Sci. Appl.* **488** (1), 215–228 (1989).
11. Salman, N. S. & Alshamsi, H. A. Synthesis of sulfonated polystyrene-based porous activated carbon for organic dyes removal from aqueous solutions. *J. Polym. Environ.* **30**, 5100–5118 (2022).
12. Usmanov, D. et al. Direct detection of morphine in human urine by surface-ionization mass spectrometry. *Eur. J. Mass Spectrom.* **26** (2), 153–157 (2020).
13. Zhang, C. et al. Development of quantum dots-labeled antibody fluorescence immunoassays for the detection of morphine. *J. Agric. Food Chem.* **65**(6), 1290–1295 (2017).
14. Cao, J., Chen, X. Y. & Zhao, W. R. Determination of morphine in human urine by the novel competitive fluorescence immunoassay. *J. Anal. Methods Chem.* (2019).
15. Ke, H. et al. Detection of morphine in urine based on a surface plasmon resonance imaging immunoassay. *Anal. Methods*. **12** (23), 3038–3044 (2020).
16. Beitollai, H., Mohammadi, S. Z. & Tajik, S. Electrochemical behavior of Morphine at the surface of magnetic core shell manganese Ferrite nanoparticles modified screen printed electrode and its determination in real samples. *Int. J. Nano Dimension*. **10** (3), 304–312 (2019).
17. Akbarian, Y., Shabani-Nooshabadi, M. & Karimi-Maleh, H. Fabrication of a new electrocatalytic sensor for determination of diclofenac, morphine and mefenamic acid using synergic effect of NiO-SWCNT and 2, 4-dimethyl. N/-[1-(2, 3-dihydroxy phenyl) methylidene] aniline. *Sens. Actuators B Chem.* **273**, 228–233 (2018).
18. Sohrabi, H. et al. Patulin and trichothecene: characteristics, occurrence, toxic effects and detection capabilities via clinical, analytical and nanostructured electrochemical sensing/biosensing assays in foodstuffs. *Crit. Rev. Food Sci. Nutr.* **62** (20), 5540–5568 (2022).
19. Sanko, V. et al. An electrochemical sensor for detection of trace-level endocrine disruptor bisphenol A using Mo2Ti2AlC3 MAX phase/MWCNT composite modified electrode. *Environ. Res.* **212**, 113071 (2022).
20. Alizadeh, T. et al. Highly selective extraction and voltammetric determination of the opioid drug buprenorphine via a carbon paste electrode impregnated with nano-sized molecularly imprinted polymer. *Microchim. Acta*. **186**, 1–8 (2019).
21. Bagheri, H. et al. Sensitive and simple simultaneous determination of morphine and codeine using a zn 2 SnO 4 nanoparticle/graphene composite modified electrochemical sensor. *New J. Chem.* **40** (8), 7102–7112 (2016).
22. Navaee, A., Salimi, A. & Teymourian, H. Graphene nanosheets modified glassy carbon electrode for simultaneous detection of heroine, morphine and noscapine. *Biosens. Bioelectron.* **31** (1), 205–211 (2012).
23. Li, F. et al. Simple and rapid voltammetric determination of morphine at electrochemically pretreated glassy carbon electrodes. *Talanta*. **79** (3), 845–850 (2009).
24. Bo, X. et al. Electrochemical oxidation and detection of morphine at ordered mesoporous carbon modified glassy carbon electrodes. *Electroanal. Int. J. Devot. Fund. Pract. Aspects Electroanal.*. **21**(23), 2549–2555 (2009).
25. Starukh, H. & Praus, P. Doping of Graphitic Carbon Nitride with non-metal elements and its applications in Photocatalysis. *Catalysts*. **10**(10), 1119 (2020).
26. Wang, Q. et al. Recent advances in g-C3N4-Based materials and their application in Energy and Environmental sustainability. *Molecules*. **28**. https://doi.org/10.3390/molecules28010432 (2023).
27. Safaei, J. et al. Graphitic carbon nitride (gC 3 N 4) electrodes for energy conversion and storage: a review on photoelectrochemical water splitting, solar cells and supercapacitors. *J. Mater. Chem. A*. **6** (45), 22346–22380 (2018).
28. ul Ain, N. et al. Copper sulfide nanostructures: synthesis and biological applications. *RSC Adv.* **12** (12), 7550–7567 (2022).
29. Maheshwaran, S. et al. Copper sulfide nano-globules reinforced electrodes for high-performance electrochemical determination of toxic pollutant hydroquinone. *New J. Chem.* **45** (6), 3215–3223 (2021).
30. Lai, Q., Christian, M. & Aguey-Zinsou, K. F. Nanoconfinement of borohydrides in CuS hollow nanospheres: a new strategy compared to carbon nanotubes. *Int. J. Hydrog. Energy*. **39** (17), 9339–9349 (2014).
31. Chung, J. S. & Sohn, H. J. Electrochemical behaviors of CuS as a cathode material for lithium secondary batteries. *J. Power Sources*. **108** (1–2), 226–231 (2002).
32. Saranya, M. et al. Hydrothermal growth of CuS nanostructures and its photocatalytic properties. *Powder Technol.* **252**, 25–32 (2014).
33. Mashhadizadeh, M. H., Ghalkhani, M. & Sohouli, E. Synthesis and characterization of N-MPG/CuS flower-like/MXene to modify a screen-printed carbon electrode for electrochemical determination of nalbuphine. *J. Electroanal. Chem.* **957**, 118130 (2024).
34. Zou, J. et al. A hydroquinone sensor based on a new nanocrystals modified electrode. *J. Chem. Technol. Biotechnol.* **89**(2), 259–264 (2014).
35. Yuan, C. et al. Flower-like copper sulfide-decorated boron-nitrogen co-doped carbon-modified glassy carbon electrode for selective and sensitive electrochemical detection of nitrobenzene in natural water. *Colloids Surf., a*. **675**, 132011 (2023).
36. Alshahrani, L. A. et al. 3D-flower-like copper sulfide nanoflake-decorated carbon nanofragments-modified glassy carbon electrodes for simultaneous electrocatalytic sensing of co-existing hydroquinone and catechol. *Sensors* **19**(10), 2289 (2019).

37. Qin, N. et al. An efficient strategy for the fabrication of CuS as a highly excellent and recyclable photocatalyst for the degradation of organic dyes. *Catalysts*. **10** (1), 40 (2019).
38. Sun, Y. et al. Ultrasensitive determination of sulfathiazole using a molecularly imprinted electrochemical sensor with CuS microflowers as an electron transfer probe and Au@ COF for signal amplification. *Food Chem.* **332**, 127376 (2020).
39. Zahran, M. et al. Recent advances in silver nanoparticle-based electrochemical sensors for determining organic pollutants in water: a review. *Mater. Adv.* **2** (22), 7350–7365 (2021).
40. Ivanišević, I. The role of silver nanoparticles in electrochemical sensors for aquatic environmental analysis. *Sensors*. **23** (7), 3692 (2023).
41. Baghayeri, M. et al. Introducing an electrochemical sensor based on two layers of Ag nanoparticles decorated graphene for rapid determination of methadone in human blood serum. *Top. Catal.* **65** (5), 623–632 (2022).
42. Hamza, A., Alshamsi, H. & Novel. Z-Scheme g-C_3N_4/TiO_2/$NiCo_2O_4$ Heterojunctions for Efficient Photocatalytic Degradation of Rhodamine B under Visible Light Irradiation. *J. Cluster Sci.* **35**(7), 2539–2556 (2024).
43. Beitollahi, H. et al. Screen-printed graphite electrode modified with graphene-Co_3O_4 nanocomposite: voltammetric assay of morphine in the presence of diclofenac in pharmaceutical and biological samples. *Nanomaterials*. **12**(19), 3454 (2022).
44. Ghalkhani, M. et al. Preparation of Mxene-AuNPs/TGA nanocomposites explored as an electrochemical aptasensor for Digoxin analysis. *Microchem. J.* **205**, 111196 (2024).
45. Nasir, K. H. & Alshamsi, H. A. Photocatalytic degradation of rhodamine B using $ZnCo_2O_4$/N-doped g-C_3N_4 nanocomposite. *J. Inorg. Organomet. Polym Mater.* 1–18 (2024).
46. Al-nayili, A., Khayoon, H., Alshamsi, H. & Saady, N. C. A novel bimetallic (Au-Pd)-decorated reduced graphene oxide nanocomposite enhanced rhodamine B photocatalytic degradation under solar irradiation. *Mater. Today Sustain.* **24**, 100512 (2023).
47. Albo Hay Allah, M. A. & Alshamsi, H. A. Green synthesis of ZnO NPs using Pontederia crassipes leaf extract: characterization, their adsorption behavior and anti-cancer property. *Biomass Convers. Biorefinery*. **14**, 10487–10500 (2024).
48. Allah, M. A. A. H., Ibrahim, H. K., Alshamsi, H. A. & Saud, H. R. Eco-friendly synthesis of biochar supported with zinc oxide as a heterogeneous catalyst for photocatalytic decontamination of rhodamine B under sunlight illumination. *J. Photochem. Photobiol., a*. **449**, 115413 (2024).
49. Teymourinia, H., Alshamsi, H. A., Al-Nayili, A. & Gholami, M. Photocatalytic degradation of chlorpyrifos using Ag nanoparticles-doped g-C_3N_5 decorated with dendritic CdS. *Chemosphere* **344**, 140325 (2023).
50. AL-Abayechi, M. M. H., Al-nayili, A. & Balakit, A. A. Montmorillonite clay modified by $CuFe_2O_4$ nanoparticles, an efficient heterogeneous catalyst for the solvent-free microwave-assisted synthesis of 1, 3-thiazolidin-4-ones. *Res. Chem. Intermed.* **50**, 1541–1556 (2024).
51. AL-Abayechi, M. M. H., Al-nayili, A. & Balakit, A. A. Green synthesis of 1, 3-Thiazolidin-4-ones derivatives by using acid-activated montmorillonite as catalyst. *Inorg. Chem. Commun.* **161**, 112076 (2024).
52. Al-Abayechi, M. M., Al-Nayili, A. & Balakit, A. A. & El-Hiti, G. A. Organic synthesis via renewable heterogeneous nanocatalysts based on Montmorillonite Clay. *Curr. Org. Chem.*, **28**, 213–221 (2024).
53. Al-Nayili, A. & Alhaidry, W. A. Novel surface structure of $LaFeO_3$/nitrogen-deficient g-C_3N_4 nanocomposites to improve visible-light photocatalytic performance toward phenol removal. *Environ. Sci. Pollut. Res.* **31**, 8781–8797 (2024).
54. Al-Nayili, A. & Haimd, S. A. Design of a new $ZnCo_2O_4$ nanoparticles/nitrogen-rich g-C_3N_4 sheet with improved photocatalytic activity under visible light. *J. Cluster Sci.*, **35**, 341–358 (2024).
55. Khayoon, H. A., Ismael, M., Al-nayili, A. & Alshamsi, H. A. Fabrication of $LaFeO_3$-nitrogen deficient g-C_3N_4 composite for enhanced the photocatalytic degradation of RhB under sunlight irradiation. *Inorg. Chem. Commun.* **157**, 111356 (2023).

Acknowledgements
The research study was supported by a research from the Farhangian University and University of Zanjan.

Author contributions
Hakimeh Teymourinia: Data curation; Investigation; Methodology; Software; Writing - original draft; Writing - review & editing. Zakyeh Akrami: Conceptualization; Data curation; Investigation; Writing - review & editing. Ali Ramazani: Conceptualization; Data curation; Funding acquisition; Methodology; Project administration; Resources; Supervision; Validation; Visualization; Writing - original draft; Writing - review & editing, Vahid Amani: Funding acquisition, Resources, Writing-Review & Editing.

Funding
The research study was supported by a research from the Farhangian University.

Declarations

Competing interests
The authors declare no competing interests.

Additional information
Supplementary Information The online version contains supplementary material available at https://doi.org/10.1038/s41598-024-78585-y.

Correspondence and requests for materials should be addressed to H.T.

Reprints and permissions information is available at www.nature.com/reprints.

Publisher's note Springer Nature remains neutral with regard to jurisdictional claims in published maps and institutional affiliations.